Transactions of the Korean Nuclear Society Autumn Meeting
Gyeongju, Korea, October 26-27, 2017

Dynamic Simulation Modeling and Analysis of Under-sodium Fuel during In-vessel Transfer Motions

Youn-Hee Kwon, Dong-Won Lim*, and Sung-Kyun Kim
Korea Atomic Energy Research Institute, Daedeok-daero 989-111 Yuseong-gu, Daejeon, Korea
**Corresponding author: dwlim@kaeri.re.kr*

1. Introduction

The refueling—a procedure to replace a spent or damaged nuclear fuel with fresh fuel—requires fuel handling in a reactor vessel. Most Sodium-cooled Fast Reactors (SFRs) employ an in-vessel transfer machine (IVTM) [1]. Because the sodium used as a coolant for SFRs reacts with air and water, refueling is performed with the reactor lid closed except early experimental or small reactors. Therefore, IVTM carries a fuel assembly (FA) under sodium, and motions in sodium cause adverse effects on the system due to viscous hydrodynamic forces on an FA. An excessive viscous force due to a fast motion is not desirable in considerations of position accuracy and structural damage on both the IVTM gripper and FA. In this paper, we deal with the dynamic behavior of an FA transferred by an IVTM under the sodium fluid. To this end, an efficient dynamic simulation model of an FA attached to the gripper in a hydrodynamic environment, reflecting fluid drag forces without applying the fluid volume (or fluid domain) in the simulation, was proposed. A commercial dynamic simulator was used for demonstration, and the test result is summarized in the end of the paper with closing remarks.

2. PGSFR Refueling System

SFR research in Korea has set out to demonstrate advancements of a Gen-IV nuclear reactor by the Prototype Gen-IV Sodium-cooled Fast Reactor (PGSFR). The PGSFR construction by 2028 had been planned, and its approval by 2020 [2].

For PGSFR, being developed by Korea Atomic Energy Research Institute (KAERI), the concept of the refueling system design is illustrated in Fig. 2. A fixed arm charge machine (FACM) used as an IVTM, being accessible to whole core FAs in combination of rotating small and large rotatable plugs (SRP and LRP, respectively), picks up an FA one by one. FACM is basically two (upper and lower) cantilever beams attached to a vertical main support column. FACM has 5 degrees of freedom: gripper jaw open/close, gripper yaw rotation, FACM yaw 360° rotation, gripper up/down, and hold-down movement to spread neighboring FAs from the target FA.

DRP is composed of SRP and LRP where SRP is offset by 680 mm from the center of LRP. The offset rotation of SRP makes FACM accessible to the whole core area by combination of LRP and FACM rotations. DRP structurally supports IVTM and other primary components such as control rod drive machine and upper internal structure.

A spent FA gripped by FACM is moved to the cask located in the upper working floor through the gate valve of the fuel transfer port (FTP) in the reactor head guided by the basket guide tube. Self-motorized EVTM, the cask carriage, provides an inert environment of the FA pathway, and goes back and forth between the reactor and fuel buildings, passing an air-lock gate.

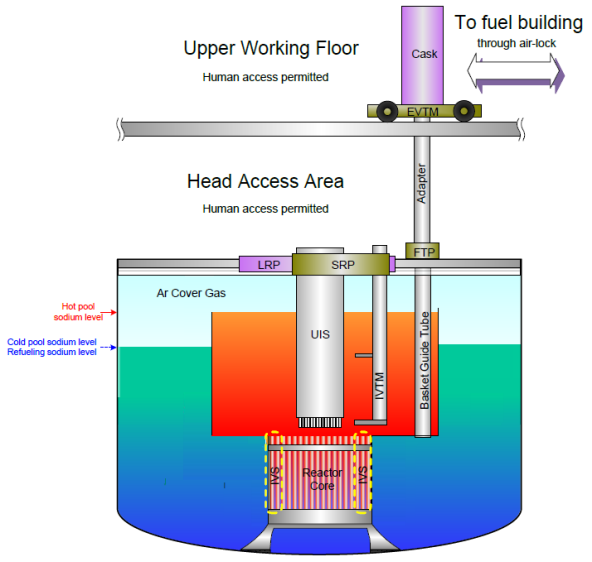

Fig. 1 The overview of PGSFR fuel handling with only IVS

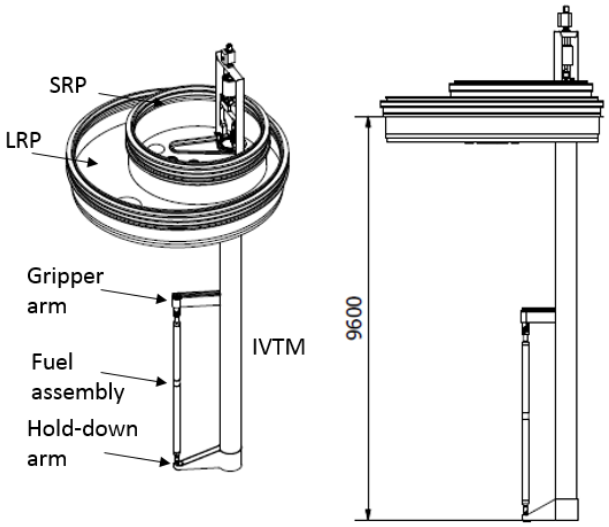

Fig. 2 PGSFR IVTM design concept

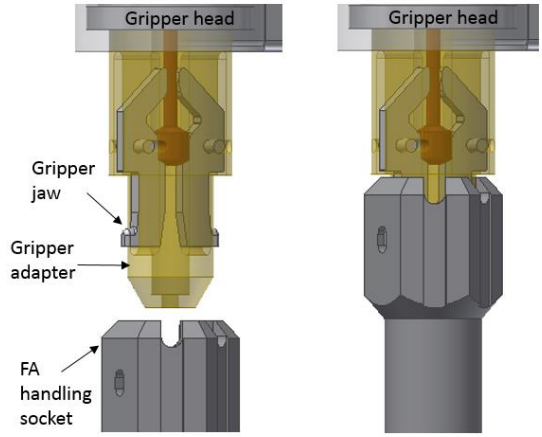

Fig. 3 FA gripper in a disengaged view (left), and FA engaged in the gripper (right)

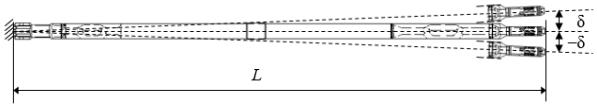

Fig. 4 FA latteral deflection

3. FA Modeling in a Hydrodynamic Environment

In order to transport an FA, IVTM uses a gripper equipped at the end of the gripper arm, and the top of an FA—the FA head—is held by the gripper jaws. The gripper mechanism is illustrated in Fig. 3. As shown, the gripper adapter is inserted into the FA handling socket at its head, and the gripper jaws are fitted into the key holes of the socket. The whole body of FA is held by its head; therefore, the FA deflection due to its motions can be described as a cantilever beam which is supported at one end as shown in Fig. 4. Its lateral deflection is mainly due to the inertia and viscous forces, and the gravity is not considered.

The relative location of the tip to the hold-down arm (or the ring, which the FA tip at rest is located in the center of) is of great concern. Considering its slow motion, the maximum deflection is at the tip, and its tip deflection δ is considered for this study as a metric of its accuracy measurement. Moreover, the extent of external forces exerted on the body can be estimated by the tip deflection.

Therefore, the FA body can be substituted as a point mass with its structural stiffness and damping elements in Fig. 5, and this spring-mass-damper system connected to the center of the hold-down ring can be modeled to demonstrate the tip deflection of an FA attached to the gripper. In other words, when the FA body is not deflected as aligned to the center line of the gripper, the red dot for the FA tip is at the center of the ring, and δ is zero.

The mass m of an FA is 296 kg, and its Young's modulus E, length L, and the cross-sectional second moment of inertia I were adopted from [3].

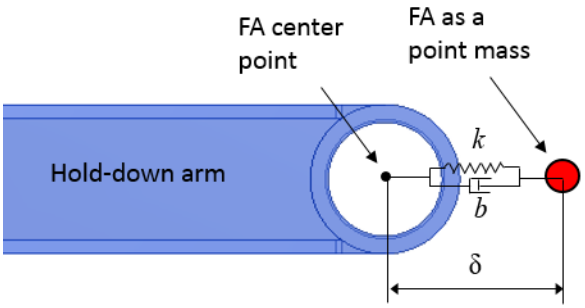

Fig. 5 FA modeling as a point mass to render the tip deflection in simulation (top view)

For a cantilever beam loaded with uniform distributed forces, the structural stiffness k can be defined by its tip deflection as

$$k = \frac{8EI}{L^3} = 52 \times 10^3 \text{ [N/m]}. \quad (1)$$

In this paper, the structural damping ratio ζ of 0.303% was taken considering typical cantilever beam structures [4]. The parameter can be precisely tuned by experimental results further in the future. Thus, the structural damping coefficient becomes

$$b = 2\zeta\sqrt{mk} = 23.83 \text{ [Ns/m]}. \quad (2)$$

With the system parameters described in the above, assuming no external forces exerted on the FA, the equation of motion for the tip deflection considering hydrodynamic forces by its lateral motions becomes

$$(m + m_a)(\ddot{x} + \ddot{\delta}) + b\dot{\delta} + k\delta + f_d = 0. \quad (3)$$

In the equation, x is the transverse location of the hold-down arm, m_a is the fluid added mass, and f_d is the drag force due to the fluid reaction. m_a and f_d are induced by hydrodynamic relations, which can be deduced by Morison's equation [5]. Define the added mass force f_a, and then

$$f_a = m_a\ddot{x} = \left(2 + \frac{8\sqrt{\nu}}{\sqrt{\pi f}L}\right)\rho_s V\ddot{x}, \quad (4)$$

$$f_d = \frac{1}{2}\left(\frac{5.93}{\sqrt{Re}} + 1.17\right)\rho_s A_P|\dot{x}|\dot{x}. \quad (5)$$

In Eqs. (4, 5), ν, f, ρ_s, V, and A_P are the kinematic viscosity of sodium, natural frequency of an FA, sodium density, FA volume, and projected frontal area, respectively.

4. Simulation Methods and Results

Among many FA transfer moves, one of the most critical transitions is from/to the core to/from the fuel transfer port (CF move). In Fig. 6., a transfer posture to be ready for an insertion to the port is shown. In the

figure, rotations of LRP and SRP are substituted by links for an easy illustration in a plane view. By three rotations of LRP, SRP and IVTM synchronously, the IVTM gripper (or the hold-down) arm can be inserted in a straight line to the port for the CF move. The simulation here only considers the CF move, and demonstrates the evaluation procedure of the deflections of an FA in a hydrodynamic environment.

To deal with hydrodynamic forces, two simulation rounds in a row are performed. The first run is a procedure to obtain positions, velocities, and accelerations of the hold-down arm for the whole discrete steps for one transfer procedure with the fixed joint to the FA. In other words, in this first simulation set, the point mass as an FA is locked, and it follows exactly the motions of the hold-down arm. After securing dynamics information of the hold-down arm, stepwise hydrodynamic forces are calculated by Eqs. (4 and 5), and are submitted for an additional input as settings at each simulation step. By running the second round of simulation for the same CF move, the deflections of the FA can be obtained, while the hold-down arm has the exactly same move with the first simulation round.

Fig 7. shows simulation results of the CF move. In this simulation, LRP rotates from 85° to 0° at the average speed of 2.36 rpm. For the straight translation of the hold-down arm (from the posture shown in Fig. 6) to the port, SRP and IVTM rotate correspondingly.

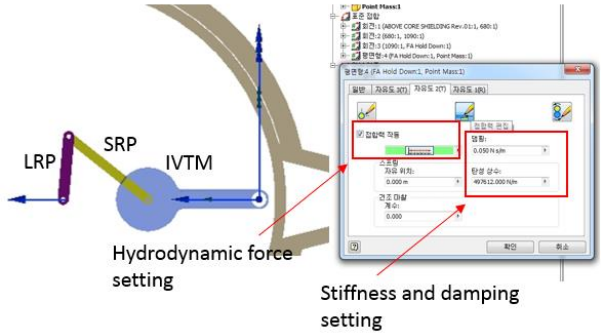

Fig. 6 Simulation setting for hydrodynamic forces induced by transfer motions

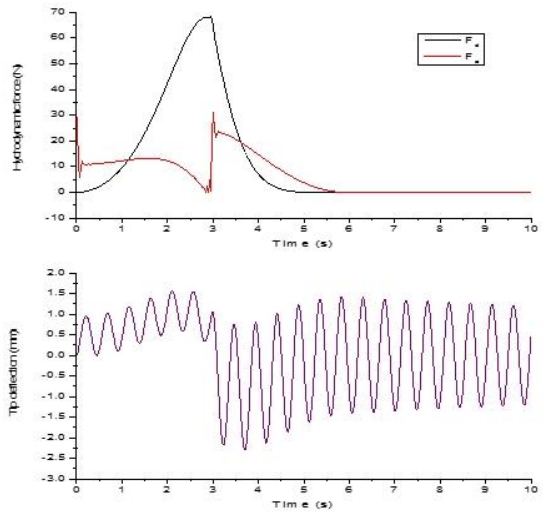

Fig. 7 Hydraulic forces induced by transfer motions (up) and corresponding tip deflections of the transferred FA (bottom)

Following the first simulation round, hydrodynamic forces are plotted in Fig. 7 (top). The blue and red curves represent a viscous drag and added mass force due to the acceleration of the fluid, respectively. As shown in the figure, the drag force gradually increases until the middle of its travel. But, as the gripper approaches to the port, its drag force shortly falls, and becomes zero when the gripper stops at about 6 seconds. The added mass force slightly fluctuates as the gripper velocity changes. As the gripper stopped, the added mass force also becomes zero. However, the FA vibration is sustained for a few more seconds due to its inertia, even after the CF move has been terminated. Because of the hydrodynamic effects, the tip of the FA sways about +/- 2.3 mm that is allowable considering the IVTM accuracy requirement of +/- 2.5 mm. Nevertheless, the speeds of actuators rotations need to be slower than the setting given in this simulation for the reliable transportation to be secured with a high margin of safety.

5. Conclusions

For the in-vessel refueling for SFRs, an FA is transferred under the sodium fluid. Motions in sodium cause viscous hydrodynamic forces on an FA. For PGSFR, the in-vessel transfer system, which employs DRP and IVTM, and its refueling procedure were briefly reviewed. For the application of FA deformations in PGSFR refueling, an efficient dynamic simulation model of an FA attached to the gripper for in-vessel transfer motions considering hydrodynamic forces was proposed as a simple spring-mass-damper system. This system is under influences of fluid-drag and -added forces due to FA motions. The simulation effectively reflected these fluid forces without the fluid volume (or fluid domain) in the setting, and so it runs effortlessly (at a low computational cost).

To this end, consecutive simulation runs were suggested in this paper. The first simulation set gives required dynamics information of the hold-down arm to calculate hydrodynamic forces, which are set on the FA for the second simulation round. Finally, the tip deflection of the transferred FA could be obtained.

A case study that the gripper enters the fuel transfer port with an average speed of 2.36 rpm LRP rotation was given for a demonstration. The hydrodynamic forces were able to be considered by the intermediate outputs as inputs for the second run, and a range of +/- 2.3 mm tip deflections was obtained. This oscillation range was within the allowable range but with a slim margin.

In the future, simulation parameters such as various speeds and dynamic factors will be considered to evaluate FA dynamics while refueling. Based on the information, a safe refueling operation—its procedure, moving trajectory, safe speed, etc.—will be determined.

ACKNOWLEDGEMENTS

This study was supported by the Ministry of Science, ICT, and Future Planning of South Korea through National Research Foundation funds (National Nuclear Technology Program, No. 2012M2A8A2025635)

REFERENCES

[1] Y. Chikazawa, M. Farmer, and C. Grandy, Technology gap analysis on sodium-cooled reactor fuel-handling system supporting advanced burner reactor development, Nuclear Technology, Vol. 165, p. 270-292, 2009.
[2] J. Yoo, J. Chang, J. Lim, J. Cheon, T. Lee, et al., Overall system description and safety characteristics of prototype Gen IV sodium cooled fast reactor in Korea, Nuclear Engineering and Technology, Vol. 48, p. 1059-1070, 2016.
[3] C. B. Lee, et al., Metal Fuel Development and Verification for Prototype Generation IV Sodium-Cooled Fast Reactor, Nuclear Engineering and Technology 48.5, p. 1096-1108, 2016.
[4] N. W. Hagood, and F. Andreas, Damping of structural vibrations with piezoelectric materials and passive electrical networks, Journal of Sound and Vibration 146.2 p. 243-268, 1991.
[5] B. M. Sumer, Hydrodynamics around cylindrical structures, Vol. 26. World scientific, 2006.